

Thermotropic Nematic and Smectic Order in Silica Glass Nanochannels

Andriy V. Kityk^{11, a)} and Patrick Huber²¹

¹*Faculty of Electrical Engineering, Czestochowa University of Technology, Aleja Armii Krajowej 17, 42-200 Czestochowa, Poland*

²*Experimental Physics, Saarland University, D-66041 Saarbruecken, Germany*

(Dated: 5 February 2022)

Optical birefringence measurements on a rod-like liquid crystal (8OCB), imbibed in silica channels (7 nm diameter), are presented and compared to the thermotropic bulk behavior. The orientational and positional order of the confined liquid evolves continuously at the paranematic-to-nematic and sizeably broadened at the nematic-to-smectic order transition, resp., in contrast to the discontinuous and well-defined second-order character of the bulk transitions. A Landau-de-Gennes analysis reveals identical strengths of the nematic and smectic ordering fields (imposed by the walls) and indicates that the smectic order is more affected by quenched disorder (originating in channel tortuosity and roughness) than the nematic transition.

The properties of spatially nano-confined liquid crystals (LCs) can be altered markedly compared to their bulk behavior¹⁻⁸. For example, high-resolution calorimetry revealed that the heat capacity anomaly in the vicinity of the second-order nematic-to-smectic-A (N-A) phase transition (PT), being evidently seen in the bulk, is absent or at least significantly broadened upon confinement in aerogels². Similarly, at temperatures T even far above the bulk isotropic-to-nematic (I-N) PT there exists often a weak residual nematic ordering, a paranematic (PN) state⁷, which can be rigorously demonstrated by optical birefringence measurements performed on nematogen LCs confined in mesopores⁸.

In this Letter we report an optical birefringence study on octyloxycyanobiphenyl (8OCB) confined in a mesoporous silica membrane permeated by parallel-aligned nanochannels (denoted as p-SiO₂). As we demonstrate here, it is especially suitable for optical polarization studies both on the orientational and positional molecular ordering of nano-confined LCs. Moreover, its straight tubular pore topology renders p-SiO₂ particularly interesting for fundamental studies on spatially confined condensed matter systems aimed at a comparison of theory and experiment, as we shall demonstrate by a comparison of our results with a Landau-de-Gennes model for nematic and smectic order in cylindrical geometry.

p-SiO₂ has been prepared by electrochemical, anodic etching of highly doped *p*-type <100> oriented silicon wafers. The membranes of $\sim 300 \mu\text{m}$ thickness have been subjected to thermal oxidation for 12 hours at $T = 800 \text{ }^\circ\text{C}$ under standard atmosphere. The obtained monolithic SiO₂ membranes are permeated by channels perpendicular-aligned to the surface. The average pore diameter is 7 nm and the porosity is $\sim 48 \%$, as determined by recording a N₂ sorption isotherm at $T = 77 \text{ K}$. The p-SiO₂ substrates were completely filled by spontaneous imbibition with 8OCB in the isotropic phase^{10,11}. For the bulk measurements the sample cell, made of parallel glass plates ($d=50 \mu\text{m}$), has been filled by the LC in

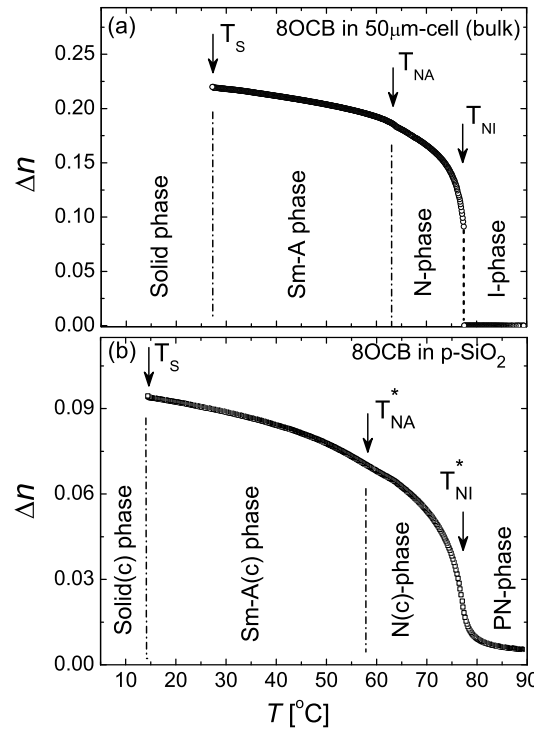


FIG. 1. Measured optical birefringence Δn vs. temperature T for 8OCB in the bulk state (a) and confined in 7 nm pores of p-SiO₂ (b).

an homeotropically aligned state. The optical birefringence measurements were performed at a wavelength λ of 632.8 nm on samples tilted out with regard to their optical axis (coinciding with the channel's long axes) by 43 deg. The high-resolution optical polarization setup employs a photoelastic modulator and a dual lock-in detection scheme in order to minimize the effects of uncontrolled light-intensity fluctuations^{8,12}. The accuracy of the optical retardation measurements is better than 5×10^{-3} deg. The optical birefringence calculated therefrom is a direct measure of the orientational (nematic) order parameter (OP) of the LC, the director. Moreover, it is also sensitive to the smectic OP, as we will discuss in more detail

^{a)} E-mail: andriy.kityk@univie.ac.at, p.huber@physik.uni-saarland.de

below.

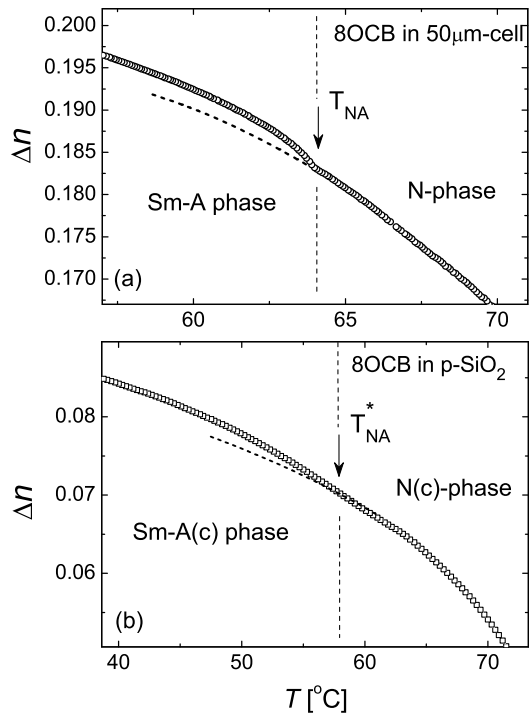


FIG. 2. Expanded plots of the temperature-dependent birefringence $\Delta n(T)$ in the regime of the nematic-to-smectic transition: (a) bulk, (b) confined in p-SiO₂.

In Fig. 1 we show the optical birefringence of 80CB measured upon slow cooling (~ 0.01 K/min) to the solidification temperature T_S in the bulk and the nanoconfined states. Upon lowering T , bulk 80CB exhibits three PTs: the I-N PT at $T_{IN} \approx 77$ °C, the N-A PT at $T_{NA} \approx 63.5$ °C and the smectic-A-to-crystalline PT at $T_S \approx 27.0$ °C. The overall shape of the $\Delta n(T)$ -dependence is in good agreement with earlier studies of Beaubois and Marcerou¹³. However, due to the considerably higher resolution our measurements describe more precisely the characteristics of the N-A PT. It is continuous as one can infer from the expanded plot in Fig. 2 (a) and from an extrapolation (dashed line below T_{NA}) of the much stronger increase in δn typical of the orientational ordering gradually evolving below T_{IA} .

The LC confined in p-SiO₂ exhibits a considerably different T -behavior, see Fig. 1 (b). The nematic ordering does not occur here via a discontinuous, first-order PT, but is clearly continuous in the vicinity of the bulk PT point T_{IN} . Moreover, at temperatures even above T_{IN} there exists a weak residual nematic ordering characteristic of a paranematic state, documented by a specific pre-transitional tail in the measured birefringence. Also the kink in the $\Delta n(T)$ dependence related with the second-order nematic-to-smectic-A PT, seen in bulk 80CB, appears to be substantially smeared out upon confinement in p-SiO₂, see Fig. 2.

A further description of the confinement effects re-

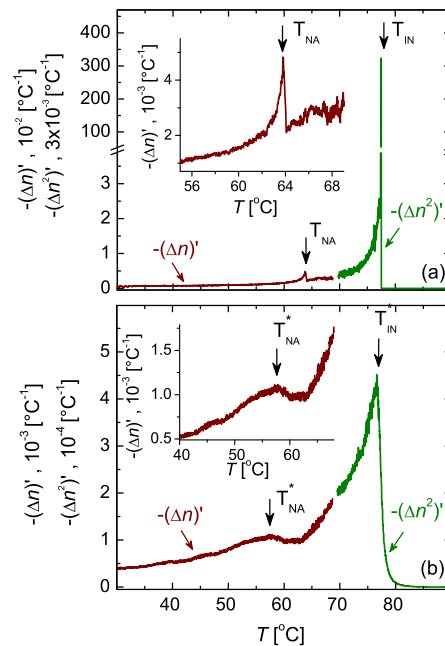


FIG. 3. Derivatives $(\Delta n)'$ and $(\Delta n^2)'$ vs. temperature as determined from the data shown in Fig. 1. (a) bulk, (b) confined in p-SiO₂.

quires the definition of the characteristic temperatures which separate the PN from the nematic (N) state ($T = T_{IN}^*$) or the N and Smectic-A (Sm-A) states ($T = T_{NA}^*$). One should be aware that both T_{IN}^* and T_{NA}^* have not any more a character of a PT in a classic meaning, since there is no spontaneous symmetry breaking in their vicinity. The full rotational symmetry is broken already by the anisotropic spatial confinement. Nevertheless, most of the physical properties keep anomalous behavior. As has been demonstrated in previous studies^{3,4,9?} the peak position of the heat capacity anomaly, $C_p(T)$, is a legitimate indicator for a definition of the PT temperatures. Moreover, anomalous behavior is also exhibited by the T -derivative of the OP squared, $d\eta^2/dT$, being proportional to $-T^{-1}C_p(T)$. Hence, taking into account that Δn is proportional to the orientational (nematic) OP, Q , and is quadratic with respect to the positional (smectic) OP, S , the temperature derivatives $(\Delta n^2)' = d(\Delta n^2)/dT$ and $(\Delta n)' = d(\Delta n)/dT$ are suitable for an accurate determination of the PT temperatures. In Fig. 3 we present the T -dependences of these derivatives extracted from the measured birefringence of 80CB in the bulk and in the nanoconfined state. It is obvious that confinement leads to a considerable broadening of the derivative peaks, in accordance with previous calorimetry and diffraction studies on calamitic LCs confined in mesopores^{4,5,9}.

In the following we analyze the obtained results with a Landaude-Gennes model for the I-N and N-A PTs. The surface of amorphous silica pores enforce planar anchoring without a preferred in-plane direction¹. However, the elongated geometry of cylindrical pores yields a preferred

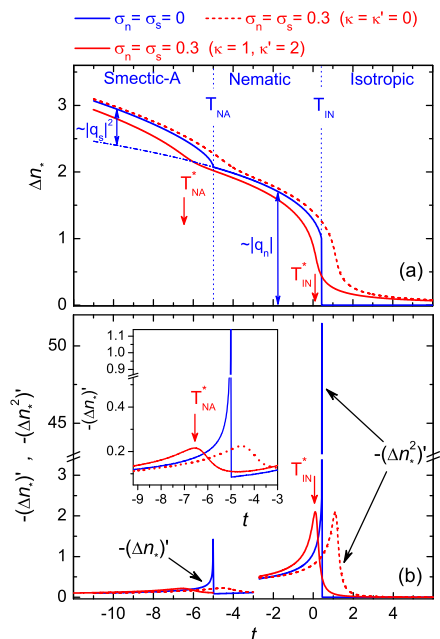


FIG. 4. Calculated normalized birefringence Δn^* vs. reduced temperature t (a) and t -derivatives $(\Delta n^*)'$ and $(\Delta n^{*2})'$ vs. t (b) for selected surface field and quenched disorder parameters.

ordering along the pore axes. The dimensionless free energy density f relevant to nematic (f_n) and smectic (f_s) ordering for such a geometry reads as⁴:

$$\begin{aligned}
 f &= f_n + a f_s, \\
 f_n &= t_n q_n^2 - 2q_n^3 + q_n^4 + c q_n^6 - q_n \sigma_n + \kappa_s q_s^2, \\
 f_s &= t_s q_s^2 + \frac{1}{2} q_s^4 + c' q_s^6 - q_s \sigma_s + \kappa_n q_n^2
 \end{aligned}
 \quad (1)$$

where q_n and q_s are the normalized nematic and smectic order parameters, t_n and t_s are nematic and smectic dimensionless reduced temperatures, σ_n and σ_s are the effective nematic and smectic ordering surface fields, respectively. A more detailed description of these models can be found in Ref.⁴. The free energy expansion (1) is completed by κ_n - and κ_s -terms describing quenched disorder effects, originating from random orientational and positional field contributions, whereas the six order c - and c' -terms are included in order to reproduce the gradual saturation of the OP at low T .

Minimization of the free energy (1) with respect to the OP q_n and q_s gives their equilibrium magnitudes $|q_n|$ and $|q_s|$. Due to the specific coupling between the optical electromagnetic wave, represented by the displacement vector $\vec{D}(\omega, k)$, and the OPs q_n and q_s , which reads as $\vec{D}_i(\omega, k) \vec{D}_i^*(\omega, k) q_n$ and $\vec{D}_i(\omega, k) \vec{D}_i^*(\omega, k) q_s^2$, resp., the measured Δn scales with $|q_n|$ and $|q_s|^2$. In Fig. 4 we show the normalized birefringence $\Delta n^* = \Delta n(T)/\Delta n(T_{IN})$ and its t -derivatives $(\Delta n^*)'$ and $(\Delta n^{*2})'$ vs. the reduced temperature t being calculated for different sets

of free energy parameters. For vanishing surface fields (blue line) the model yields discontinuous behavior and describes the overall behavior in very good agreement with our observation for the bulk system. In order to reproduce the continuous behavior in the pores, we had to use final, but identical values for the strength of the nematic and smectic ordering fields (see Fig. 3), and arrive thereby at a good description of all main features observed, including the PN ordering and broadening of the temperature peaks of the derivatives $(\Delta n)'$ and $(\Delta n^2)'$ in the vicinity of T_{IN}^* and T_{NA}^* . Moreover, in order to account for the unshifted T_{IN}^* and significantly downshifted T_{NA}^* (by ~ 6 °C), we have to use $\kappa_s = 2\kappa_n = 1$ for the influence of quenched disorder on the smectic and nematic transition. Thus, a final tortuosity and pore wall roughness, presumably responsible for the quenched disorder contributions^{1,8}, affect the layering formation significantly stronger than the evolution of orientational order¹⁴.

Finally it is interesting to note that upon entering into the N-phase the bulk shear viscosity of 8OCB exhibits a minimum, resulting from an abrupt collective shear-alignment of the molecules. This rheological feature is, however, absent in silica mesopores, as was recently demonstrated by capillary filling experiments¹¹. We believe the very gradual (and not abrupt) evolution of the nematic ordering upon nano-channel confinement, documented here, is responsible for this peculiarity. Thus, our study sheds not only important light on the equilibrium positional and orientational order of an archetypical rod-like LC, it allows also for a better understanding of the non-equilibrium behavior of this system upon nano-confinement.

- ¹G.P. Crawford and S. Zumer (Eds.), Liquid Crystals in Complex Geometries, Taylor & Francis (1996).
- ²T. Bellini, L. Radzihovsky, J. Toner, and N. A. Clark, Science **294**, 1074 (2001).
- ³Z. Kutnjak, S. Kralj, G. Lahajnar, and S. Zumer, Phys. Rev. E **68**, 021705 (2003).
- ⁴Z. Kutnjak, S. Kralj, G. Lahajnar, and S. Zumer, Phys. Rev. E **70**, 051703 (2004).
- ⁵R. Guegan, D. Morineau, C. Loverdo, W. Beziel, and M. Guendouz, Phys. Rev. E **73**, 011707 (2006).
- ⁶K. Binder, J. Horbach, R. Vink, and A. de Virgiliis, Soft Matter **4**, 1555 (2008).
- ⁷J. M. Fish and R. L. C. Vink, Phys. Rev. Lett. **105**, 147801 (2010).
- ⁸A. V. Kityk, M. Wolff, K. Knorr, D. Morineau, R. Lefort, and P. Huber, Phys. Rev. Lett. **101**, 187801 (2008).
- ⁹Z. Kutnjak, S. Kralj, and S. Zumer, Phys. Rev. E **66**, 041702 (2002).
- ¹⁰P. Huber, S. Grüner, C. Schäfer, K. Knorr, and A. V. Kityk, Europ. Phys. J. Spec. Top. **141**, 101 (2007).
- ¹¹S. Gruener and P. Huber, arXiv:1005.0730.
- ¹²M. Skarabot, M. Cepic, B. Zeks, R. Blinc, G. Heppke, A. V. Kityk, and I. Musevic, Phys. Rev. E **58** 575 (1998).
- ¹³F. Beabois and J. P. Marcerou, Europhys. Lett. **36** 111 (1996).
- ¹⁴Note that a full-fitting of the experimental results with the model is hampered by the neglect of higher order terms in Eq. 1 necessary to describe the correct saturation of the OP.